Title

Cadmium and arsenic override NF-κB developmental regulation of the intestinal UGT1A1 gene and control of hyperbilirubinemia

Authors

Liu, Miao
Chen, Shujuan
Yueh, Mei-Fei
et al.

Publication Date

2016-06-01

DOI

10.1016/j.bcp.2016.04.003

Peer reviewed

HHS Public Access

Author manuscript

Biochem Pharmacol. Author manuscript; available in PMC 2017 June 15.

Published in final edited form as:

Biochem Pharmacol. 2016 June 15; 110-111: 37–46. doi:10.1016/j.bcp.2016.04.003.

Cadmium and arsenic override NF-κB developmental regulation of the intestinal *UGT1A1* gene and control of hyperbilirubinemia

Miao Liu[a,b], **Shujuan Chen**[a], **Mei-Fei Yueh**[a], **Ryoichi Fujiwara**[a], **Camille Konopnicki**[a], **Haiping Hao**[b], and **Robert H. Tukey**[a,*]

[a]Laboratory of Environmental Toxicology, Departments of Chemistry & Biochemistry and Pharmacology, University of California, San Diego, La Jolla, CA 92023, United States

[b]State Key Laboratory of Natural Medicine, Key Laboratory of Drug Metabolism and Pharmacokinetics, China Pharmaceutical University, Nanjing, People's Republic of China

Abstract

Humanized UDP-glucuronosyltransferase (*UGT*)-*1* (*hUGT1*) mice encode the *UGT1* locus including the *UGT1A1* gene. During neonatal development, delayed expression of the *UGT1A1* gene leads to hyperbilirubinemia as determined by elevated levels of total serum bilirubin (TSB). We show in this report that the redox-sensitive NF-κB pathway is crucial for intestinal expression of the *UGT1A1* gene and control of TSB levels. Targeted deletion of IKKβ in intestinal epithelial cells (*hUGT1/Ikkβ*$^{\Delta IEC}$ mice) leads to greater neonatal accumulation of TSB than observed in control *hUGT1/Ikk*β$^{\Delta F/F}$ mice. The elevation in TSB levels in *hUGT1/Ikkβ*$^{\Delta IEC}$ mice correlates with a reduction in intestinal UGT1A1 expression. As TSB levels accumulate in *hUGT1/Ikkβ*$^{\Delta IEC}$ mice during the neonatal period, the increase over that observed in *hUGT1/Ikkβ*$^{F/F}$ mice leads to weight loss, seizures and eventually death. Bilirubin accumulates in brain tissue from *hUGT1/Ikkβ*$^{\Delta IEC}$ mice inducing an inflammatory state as shown by elevated TNFα, IL-1 β and IL-6, all of which can be prevented by neonatal induction of hepatic or intestinal UGT1A1 and lowering of TSB levels. Altering the redox state of the intestines by oral administration of cadmium or arsenic to neonatal *hUGT1/Ikkβ*$^{F/F}$ and *hUGT1/Ikkβ*$^{\Delta IEC}$ mice leads to induction of UGT1A1 and a dramatic reduction in TSB levels. Microarray analysis following arsenic treatment confirms upregulation of oxidation-reduction processes and lipid metabolism, indicative of membrane repair or synthesis. Our findings indicate that the redox state in intestinal epithelial cells during development is important in maintaining *UGT1A1* gene expression and control of TSB levels.

Keywords

UDP-glucuronosyltransferase 1A1; Humanized *UGT1* mice; Intestinal IKKβ; Oxidative stress; Bilirubin; Inflammation

*Corresponding author at: UC San Diego, 9500 Gilman Drive, Room 211, Leichtag Biomedical Research Building, La Jolla, CA 92093-0722, United States. rtukey@ucsd.edu (R.H. Tukey).

Author contributions

M.L., S.C., M.-F.Y., R.F., C.K. and R.H.T. designed research; M.L., R. F., C.K. performed research; H.H., R.H.T. contributed reagents; M.L., R.H.T. analyzed data; M.L., M.-F.Y. and R.H.T. wrote the paper.

Competing financial interests

The authors declare no competing financial interests.

1. Introduction

Neonatal jaundice (hyperbilirubinemia) is characterized by elevated levels of total serum bilirubin (TSB) and occurs in 50%–60% of newborn children and to a greater extent in premature infants [1–3]. While jaundice is normally benign, high levels of TSB can lead to the onset of chronic bilirubin encephalopathy (kernicterus), which is displayed clinically with abnormal motor control and muscle tone, oculomotor disturbances and hearing abnormalities [4]. Kernicterus results from saturating levels of unconjugated bilirubin (UCB) in the CNS being deposited or crystallized in brain tissue, a phenomenon that leads to yellow staining of selective nuclei and which is felt to underlie the icteric related behaviors associated with abnormal motor control and auditory disturbances [4–6]. Milder forms of kernicterus show more subtle CNS disabilities which are classified as bilirubin induced neurological dysfunction (BIND) [6] and do not usually encompass the more severe clinical symptoms associated with classical kernicterus. Since circulating bilirubin is metabolized selectively by UDP-glucuronosyltransferase 1A1 (UGT1A1) [7], the formation of the glucuronide is the rate limiting step leading to the elimination of bilirubin. Thus, it is believed that neonatal jaundice, BIND and the symptoms associated with kernicterus result from a developmental delay in the expression of the *UGT1A1* gene. However, clear understandings of the cellular and molecular events that control the homeostatic levels of TSB have not been elucidated.

We have demonstrated that mice humanized with the *UGT1* locus (*hUGT1* mice) and the *UGT1A1* gene develop neonatal hyperbilirubinemia [8]. In the majority of neonatal *hUGT1* mice, the accumulation of TSB and UCB is not severe enough to cause CNS toxicity. However, up to 10% of all *hUGT1* neonatal mice accumulate higher levels of TSB and develop severe motor and balance dysfunction and progress into grand mall seizures approximately two weeks after birth. Since these *hUGT1* mice accumulate high levels of bilirubin in brain tissue and display physical signs that have been documented in children with chronic bilirubin induced encephalopathy, *hUGT1* mice have been used to study the mechanism(s) associated with the onset of kernicterus [9].

The icteric condition develops in part as a result of repressed expression of hepatic UGT1A1 in neonatal *hUGT1* mice [8,10], which is linked to *UGT1A1* gene silencing by the pregnane X receptor (PXR) [10]. In the absence of adequate liver UGT1A1 expression, TSB levels are controlled through developmental expression of UGT1A1 in extrahepatic tissues such as the gastrointestinal tract. In the intestines, this expression pattern occurs in two stages during the neonatal period. First, there are low levels of intestinal UGT1A1 that correspond with the steady accumulation of TSB through the first two weeks after birth [11]. Second, the clearance of TSB in the latter stages of the neonatal period occurs in conjunction with an increase in intestinal UGT1A1. We have shown previously that the early neonatal stages of the icteric response and the accumulation of bilirubin in *hUGT1* mice result from suppression of intestinal *UGT1A1* gene expression by breast milk feeding [11]. Placing newborn *hUGT1* on a strictly formula diet dramatically induces intestinal UGT1A1 leading to a sharp drop in the accumulating TSB levels [11]. Since oral formula treatment resulted in induction of NF-κB target genes in intestinal tissue, we predicted that IKK/NF-κB signaling

is the key mechanism for switching *UGT1A1* gene expression off or on in response to breast milk or formula feeding, respectively [11].

In this study, the discovery that breast milk suppresses intestinal *UGT1A1* gene expression led us to examine the contribution of the IKK/NF-κB pathway in controlling the icteric response in *hUGT1* mice. Since NFκB responds to redox changes, such as alterations in reactive oxygen species (ROS) or antioxidant defense mechanisms [12], we speculated that changes in intestinal UGT1A1 expression and protection of the icteric response was controlled in part by redox changes that impact on activation of NF-κB. To this end, we have tested the hypothesis that the IKK/NF-κB pathway is critical in controlling intestinal *UGT1A1* gene expression during the early phases of neonatal hyperbilirubinemia.

2. Methods and materials

2.1. Chemicals and reagents

Anti-human UGT1A1 antibody was a gift from Dr. Joseph K. Ritter (Virginia Commonwealth University, Medical College of Virginia, Richmond, VA). An IKKβ antibody was purchased from Cell Signaling Technology (USA). Primers for quantitative real-time polymerase chain reaction (Q-PCR) were commercially synthesized at Integrated DNA Technologies, Inc (San Diego, CA). Cadmium chloride hemipentahydrate (Cd), pregnenalone-16a carbonitrile (PCN), and lipopolysaccharides (LPS) were purchased from Sigma-Aldrich (St. Louis, MO).

2.2. Animals and treatments

To generate *hUGT1* mice with targeted disruption of IKKβ specifically in intestinal tissue, *hUGT1* mice (*TgUGT1*28/Ugt1*$^{-/-}$ mice) [8] were crossed first with *Ikkβ*$^{F/F}$ mice [13] and their offspring backcrossed to obtain *hUGT1/Ikkβ*$^{F/F}$ mice. Two *loxP* recombination sites flank exon 3 of the Ikkβ locus, and the inactivation of the intestinal IKKβ kinase activity was accomplished by the removal of exon 3 in the presence of the Cre-recombinase expressed from a transgenic *Villin-cre* gene (Jackson Laboratory, Bar Harbor, Maine) to create *hUGT1/βIkk*$^{F/F}$*/Vil-cre* mice (*hUGT/βIkk*$^{\Delta IEC}$). For formula feeding, 10-day old neonatal mice were placed in a 37 °C incubator without nursing, and formula (37 °C, 0.15 g/ml) was administered every 3h for 3 days. For cadmium (Cd) and arsenic (As) treatment, 10 day old mice were administered Cd (10 mg/kg) or As (10 mg/kg) by oral gavage. At the end of the planned experiments, mice were euthanized, tissues collected and briefly rinsed in ice cold 1.15% KCl. All animal experiments were carried out after approval by the University of California San Diego Institutional Animal Care program.

2.3. Bilirubin measurements

Blood was obtained from the submandibular vein, collected into an Eppendorf tube, and centrifuged at 5000 × g for 5 min. From a small sample of serum, total serum bilirubin (TSB) was measured by a Unistat Bilirubinometer (Reichert, Inc., Depew, NY).

2.4. Western blot analysis

Whole tissue lysate (25 μg) was separated on 4%-12% NuPAGE Bis-Tris polyacrylamide gels (Invitrogen, Carlsbad, CA), and the protein transferred to nitrocellulose (Millipore). Following blocking with 5% nonfat dry milk in Tris-buffered saline solution (10 mM Tris [pH 8.0], 150 mM NaCl, 0.05%Tween20) for1 h, membranes were incubated with primary anti-UGT1A1 antibody overnight at 4 °C followed by three washes with Tris-buffered saline solution. Horseradish peroxidase-conjugated secondary antibody was added at room temperature for 1 h with gentle shaking. After application of chemiluminescence reagents (Western Lightning from Perkin Elmer Life Sciences), images were obtained in a Bio-Rad Universal Hood II equipped with a ChemiDox XRS imaging system.

2.5. Reverse transcription (RT) and real time-PCR

Total RNA was isolated using TRIzol reagents according to the manufacturer's instructions (Invitrogen, Carlsbad, CA). Complementary RNA was prepared using iSCRIPT (Bio-Rad) and real time PCR was performed using SYBR master mix (Eurogentec, San Diego) with a pair of gene-specific primers and the cyclophilin (CPH) gene as an internal control gene using the CFX96 Touch Real-Time PCR Detection System (BioRad). The primers used were: UGT1A1 forward, 5′-CCATCATGCCCAATATGGTT-3′ and UGT1A1 reverse, 5′-CCACAATTCCATGTTCTC CA-3′; Mouse cyclophilin (mCPH) forward, 5′-CAGACGCCACTGTCGCTTT-3′ and mCPH reverse, 5′-TGTCTTTGGAACTTTGTCTGC AA-3′; TNFα forward, 5′-CATCTTCTCAAAATTCGAGTGACAA-3′ and TNFα reverse 5′-TGG GAGTAGACAAGGTACAACCC-3′; IL-1β forward 5′-GCAACTGTTCCT GAACTCAACT-3′ and IL-1β reverse 5′-ATCTTTTGGGGTCCGT CAACT-3′; IL-6 forward 5′-GAGGATACCACTCCCAACAGACC-3′ and IL-6 reverse 5′-AAGTGCATCATCGTTGTTCATACA-3′; IL-8 forward 5′-ATGCCCTCTATTCTGCCAGAT-3′ and IL8 reverse 5′-GTGCTCCGGT TGTATAAGATGAC-3′; COX-2 forward 5′-GCAGGATGCCACTCT GAATC-3′ and COX-2 reverse 5′-GCTCGGCTTCCAGTATTGAG-3′. Each gene analysis was performed in triplicate, normalized to the internal control gene CPH, and quantitated based on the formula $\Delta C_{\mathrm{t}}=C_{\mathrm{t}}^{(\text{tested gene})}-C_{\mathrm{t}}^{(\mathrm{CPH})}$.

2.6. Microarray analysis

Total RNA was isolated from small intestinal tissue using the RNeasy kit from Qiagen, according to the manufacturer's instructions (Qiagen, Valencia, CA). Total RNA (~2 μg per sample) was sent to UCSD's BIOGEM facility, where after RNA purity assessment, microarray analysis was performed on Illumina's MouseWG-6 v2.0 Expression BeadChip array platform that consists of more than 45,200 transcripts (Illumina, San Diego, CA). A total of ten independent arrays (5 control and 5 As-treated) were conducted. The 5 control sets of values were averaged as were the 5 arsenic treated values for each gene.

2.7. Statistical analysis

Prism software was used and data are presented as mean ± SD. Statistically significant values are indicated with $^{*}P \leq 0.05$, $^{**}P \leq 0.01$, $^{***}P \leq 0.005$. For overall survival analysis, Kaplan-Meier curves were generated as described in the Graph Pad software.

3. Results

3.1. IKKβ knock-out in intestinal epithelial cells (IECs)

Previous studies have indicated that activation of the intestinal IKK/NF-κB pathway by oral administration of formula or cadmium (Cd) led to dramatic induction of intestinal UGT1A1 expression in neonatal *hUGT1* mice [11]. To determine the role of NF-κB in the developmental regulation of intestinal human UGT1A1, we crossed *hUGT1* mice [8] with *Ikkβ*$^{F/F}$ mice and transgenic *Villin-Cre* recombinase mice to generate *hUGT1* mice with targeted knockout of intestinal IKKβ (*hUGT1/Ikkβ*$^{\Delta IEC}$ mice). The breeding pairs for these experiments were *hUGT1/Ikkβ*$^{F/F}$ mice crossed with transgenic (Tg) *UGT1/Ugt1*$^{+/-}$/*Ikk*β$^{\Delta EC}$ mice, which generated *hUGT1/βIkk*$^{\Delta IEC}$ and *hUGT1/βIkk*$^{F/F}$ mice in the same litters. Compared with their littermate control *hUGT1/Ikkβ*$^{F/F}$ mice, deletion of the 3rd exon of the *Ikkβ* locus in IECs from *hUGT1/Ikkβ*$^{\Delta IEC}$ neonates resulted in greatly reduced intestinal IKKβ mRNA levels with no detectable IKKβ protein expression (Fig. 1B and C). Because of the humanized *UGT1* background, both *hUGT1/Ikkβ*$^{\Delta IEC}$ and *hUGT1/Ikkβ*$^{F/F}$ mice accumulate TSB levels a few hours after birth (Fig. 1D), and the pattern is indistinguishable throughout the first 7 days. However, by 10 days after birth there is a dramatic increase in TSB levels in *hUGT1/Ikkβ*$^{\Delta IEC}$ mice that continue to climb through the neonatal period. The *hUGT1/Ikkβ*$^{F/F}$ mice are healthy and their TSB levels start to clear after 14 days, a pattern that is consistent with TSB levels in *hUGT1* mice [8]. In contrast, *hUGT1/Ikkβ*$^{\Delta IEC}$ mice start to lose weight (Fig. 1E), with all these mice progressing into seizures as a result of severe hyperbilirubinemia. Kaplan-Meir curves show that approximately 10% of the *hUGT1/Ikkβ*$^{F/F}$ mice die by the end of the neonatal period, a phenomenon that we had observed previously with *hUGT1* mice [8], while 100% of the *hUGT1/Ikkβ*$^{\Delta IEC}$ mice die by 20 days after birth (Fig. 1F).

When we examined expression levels of proinflammatory cytokine genes in brain tissue during the early neonatal stage and up to that period when the mice begin to show seizure, pronounced neuroinflammation with up regulation of *Tnfα, Il-1 β, Il-6* and *Cox-2* gene expression in *hUGT1/Ikkβ*$^{\Delta IEC}$ mice (Fig. 2) was consistent with elevated TSB levels. This pattern of cytokine expression in *hUGT1/Ikk*β$^{\mathrm{D\ I}EC}$ mice is similar to what we had previously observed in *hUGT1* mice that progress into seizures and show prominent signs of bilirubin accumulation or kernicterus in brain tissue [9]. The importance of this finding demonstrates that knockout of the intestinal *Ikkβ* gene in *hUGT1* mice leads to the temporal increase in TSB levels that exceed those values normally seen in *hUGT1* mice, with the end result being severe bilirubin induced neurotoxicity and kernicterus formation. Confirming that intestinal control of UGT1A1 by IKKβ is crucial in the overall clearance of bilirubin, we treated neonatal *hUGT1/Ikkβ*$^{\Delta IEC}$ mice by oral gavage with the Pregnane X Receptor (PXR) activator PCN from day-11 to day-13 after birth. This multiple treatment leads to

induction of liver *UGT1A1* gene expression as determined on day 15 with a reduction in TSB levels (Fig. 3), eliminating any signs of bilirubin induced brain toxicity (Fig. 2).

3.2. IKKβ knock-out in the IECs inhibits human UGT1A1 expression in neonatal intestine

Since TSB levels in *hUGT1/Ikkβ*$^{\Delta IEC}$ mice are elevated in comparison to *hUGT1/Ikkβ*$^{F/F}$ mice, we examined the expression levels of the *UGT1A1* gene during neonatal development. During peak TSB levels (days 12–14) there is a statistically significant reduction in intestinal UGT1A1 gene expression in *hUGT1/Ikkβ*$^{\Delta IEC}$ mice (Fig. 4). When intestinal tissue was collected from mice at 14 days after birth and analyzed by Western blot analysis for expression of UGT1A1, levels of protein expression were reduced in accordance with *UGT1A1* gene expression patterns. It is interesting to note that as TSB levels increase in *hUGT1/Ikkβ*$^{\Delta IEC}$ mice between 14 and 16 days after birth (Fig. 1D) and the average weight of the mice is decreasing (Fig. 1E), there is a dramatic increase in intestinal *UGT1A1* gene expression (Fig. 4A). It is unclear why intestinal *UGT1A1* gene expression spikes in *hUGT1/Ikkβ*$^{\Delta IEC}$ mice (day 14–16), but the increase is unable to facilitate a reduction in TSB levels.

It has been demonstrated that treatment of glial cells with bilirubin drives an inflammatory response that is linked to activation of NFκB [9,14,15], while the development of kernicterus in brain tissue of hUGT1 mice coincides with NF-κB activation [9]. Since our findings indicate that the IKK/NF-κB pathway in intestinal epithelial cells plays a key role in maintaining homeostatic/ basal levels of human *UGT1A1* gene expression during the neonatal period, we examined if increasing TSB levels during development contributed to the *UGT1A1* gene expression patterns in the small intestine through an IKK/NF-κB mechanism. To examine this possibility, *hUGT1/Ikkβ*$^{\Delta IEC}$ mice were bred to restore the murine Ugt1 background creating transgenic *UGT1/Ikkβ*$^{\Delta IEC}$ mice (*TgUGT1/ Ikkβ*$^{\Delta IEC}$ mice). *TgUGT1/Ikkβ*$^{\Delta IEC}$ mice are genetically similar to *hUGT1/Ikkβ*$^{\Delta IEC}$ but do not accumulate serum bilirubin during neonatal development. Thus, any change in *UGT1A1* gene expression would eliminate the probability of elevated bilirubin contributing to the response. When expression levels of intestinal *UGT1A1* gene expression were analyzed in *TgUGT1/Ikkβ*$^{\Delta IEC}$ mice during the neonatal period, there was a statistically significant reduction in *UGT1A1* gene expression between days 12 and 14 when compared to expression levels in *TgUGT1/Ikk*β$^{F/F}$ mice (Fig. 5). This finding suggests that the lowered *UGT1A1* gene expression in the *Ikkβ*-null mice occurs as a result of the absence of the IKK/NF-κB pathway. Since NF-κB is a redox-sensitive transcription factor [16], the balance between reactive oxygen species (ROS) and the activation of antioxidative mechanisms (AOM) appears to be crucial in constitutive regulation of intestinal UGT1A1 gene expression during development.

3.3. Control of the oxidative state in the intestines is important for UGT1A1 expression

The absence of NF-κB, which is an important redox-sensing mechanism in intestinal epithelial cells [17,18], indicates that an imbalance in ROS/AOM may contribute to intestinal UGT1A1 gene expression in *hUGT1/Ikkβ*$^{\Delta IEC}$ mice. To examine this possibility, we treated neonatal *hUGT1/Ikkβ*$^{\Delta IEC}$ mice with cadmium (Cd) by oral gavage. Cadmium is a bivalent cation and unable to generate free radicals directly [19]. However, the generation

of ROS can occur secondarily since Cd has a high affinity for thiols, such as found with glutathione [20], thus disturbing the oxidized/reduced environment of the cell. Other forms of ROS following Cd exposure may occur through Cd disruption of mitochondrial oxidative phosphorylation, or Cd induced NADPH oxidase activity [21]. To counter or minimize ROS production, Cd exposure can lead to the activation of strong antioxidative mechanisms, many of which are displayed in signaling cascades that lead to transcriptional activation of cellular defense mechanisms.

When we treated 10 day old *hUGT1/Ikkβ*$^{\Delta IEC}$ and *hUGT1/Ikkβ*$^{F/F}$ mice orally with 10 mg/kg Cd, TSB levels dropped dramatically by the time the mice were 12 days old (Fig. 6A). Analysis of intestinal and liver *UGT1A1* gene expression demonstrated that Cd induced intestinal *UGT1A1*, but had no effect on liver *UGT1A1* gene expression (Fig. 6C and D). While a disturbed redox balance is proposed to occur following Cd exposure, the role of NF-κB in sensing this disturbance has a limited role in the control of *UGT1A1* gene expression, since comparable levels of expression are noted in both *hUGT1/Ikkβ*$^{\Delta IEC}$ and *hUGT1/Ikkβ*$^{F/F}$ mice. However, when we measured anti-inflammatory cytokine markers such as Tnfα and Il-1β, Cd treatment led to a statistically significant reduction in both cytokines in IECs isolated from *hUGT1/Ikkβ*$^{\Delta IEC}$ and *hUGT1/Ikkβ*$^{F/F}$ mice (Fig. 7A and B). The reduction in these cytokines by Cd indicates that strong antioxidative mechanisms have been induced, since the induction of Tnfα and Il-1β by chemical treatment is often linked to an inflammatory reaction associated with the production of ROS [22]. When we examined antioxidative sensitive gene expression, such as the *Gsta1* and *Gsta2* genes, both were induced in IECs following Cd exposure (Fig. 7C and D). It is also interesting to note that Cd treatment and lowering of TSB values in *hUGT1/Ikkβ*$^{\Delta IEC}$ mice rescues these mice from bilirubin toxicity, since over 95% of the treated mice show no signs of toxicity and grow without incidence into adult mice (Fig. 6B).

Arsenic is a potent inducer of oxidative stress [23–26]. As a second agent to evaluate the potential of oxidative stress in modulating intestinal UGT1A1 and TSB levels, *hUGT1/Ikkβ*$^{\Delta IEC}$ and hUGT1/ *Ikkβ*$^{F/F}$ mice that were 10-days old were treated by the oral route with 10 mg/kg arsenic. After 24 h, the TSB levels dropped in *hUGT1/Ikkβ*$^{\Delta IEC}$ and *hUGT1/Ikkβ*$^{F/F}$ mice that corresponded to induction of intestinal UGT1A1 (Fig. 8). Since this response was rapid and dramatic, we elected to carryout gene expression profiling studies using microarray analysis. Mice (*hUGT1/Ikkβ*$^{F/F}$) were treated with oral As and intestinal RNA isolated 24 h later. We carried out the gene analysis profiling with RNA samples isolated from 5 vehicle treated and 5 As treated mice. Microarray analysis was conducted individually on each sample, and the results from each group combined for final analysis.

A heat map of induced gene expression patterns is shown in Fig. 9. Over 145 genes were induced greater than 2-fold. One of the remarkable observations is the dramatic induction of oxidative genes such as the CYPs. Such a response may in part play a role in an ROS response. When the expression patterns are grouped by metabolic ontology, some of the robust profiles are those encoding oxidative-reductive processes and lipid and fatty acid metabolism (Table 1). These processes could be linked to membrane synthesis, implying membrane repair or cellular proliferation is being engaged by As treatment.

4. Discussion

Several lines of evidence using *hUGT1* mice indicate that the intestinal tract plays an important role in the homeostatic balance of serum bilirubin during neonatal development. When the *Ugt1* locus is rendered non-functional in mice by interruption of the common exons (*Ugt1*$^{-/-}$ mice), unconjugated bilirubin rapidly accumulates resulting in severe hyperbilirubinemia, CNS toxicity and death within 5–7 days after the birth of *Ugt1*$^{-/-}$ mice [27]. The accumulating bilirubin concentration in the brain leads to a disturbed redox status that triggers Toll-like receptor 2 (TRL2) signaling to provide a defense mechanism that involves the activation of glia cells [9]. If TSB levels are not reduced early in development, the inflammatory state created leads to disruption of myelination [28], which we believe underscores the seizure paradigm that develops. This lethality can be rescued by expression of the human *UGT1* locus and the *UGT1A1* gene in *hUGT1* mice [8], with a steady decline in TSB levels occurring in a developmental fashion during the later stages of the neonatal window (days 12–21). In neonatal *hUGT1* mice, the human *UGT1A1* gene is repressed in the liver during development by PXR [10] resulting in minimal expression of UGT1A1 [29]. In the absence of hepatic driven clearance of bilirubin by UGT1A1 dependent glucuronidation, extrahepatic mechanisms facilitating bilirubin glucuronidation serve to compensate for lack of liver UGT1A1 expression. We have demonstrated that as TSB levels rise during the first two weeks followed by plasma clearance of bilirubin these patterns are concordant with expression of intestinal UGT1A1 [11]. These findings indicate that the early increase in hyperbilirubinemia is controlled in part by intestinal UGT1A1 expression. Indeed, if we selectively induce intestinal *UGT1A1* gene expression during the early developmental phase when TSB levels are accumulating, the increase in hyperbilirubinemia can be rapidly reversed. Additional findings have demonstrated that direct knockout of the liver Ugt1a1 gene (*Ugt1*$^{\Delta HEP}$ mice) by loxP recombination and deletion of exons 3 and 4 is not a lethal mutation [30], confirming that metabolism of bilirubin during development can occur by extrahepatic UGT1A1 sources. Combined, these results indicate that changes in intestinal UGT1A1 gene expression are controlled early in neonatal development with these changes having an impact on bilirubin metabolism and clearance.

In previous experiments, we had demonstrated that substituting breast milk with formula led to induction of intestinal UGT1A1 and reduction in TSB levels in neonatal *hUGT1* [11]. Based upon these findings, we had speculated intestinal IKK/NF-κB was being controlled by unknown factors present in breast milk which had a direct impact on intestinal *UGT1A1* gene expression. Since NF-κB can be regulated by the intracellular redox state [12], that is the balance between ROS production and the development of antioxidant defenses, we reasoned that changes in the redox state would lead to targeted regulation of the *UGT1A1* gene. Since it has been shown previously that the IKKβ subunit of the IKK complex is responsible for activation of NFκ B in response to proinflammatory stimuli [17,31], we examined the expression pattern of the intestinal UGT1A1 gene from *hUGT1* mice that were deficient in intestinal IKKβ activity. Indeed, when regulation of NFκB was impaired in IECs by targeted knockout of the *Ikkβ* gene, intestinal expression levels of the UGT1A1 gene in *hUGT1/Ikkβ*$^{\Delta IEC}$ mice as determined by real-time PCR analysis were statistically lower than in *hUGT1/ Ikkβ*$^{F/F}$ mice. This reduced UGT1A1 gene expression in *hUGT1/* Ikkβ$^{\Delta IEC}$

mice led to greater accumulation of TSB levels early in neonatal development which promoted the onset of bilirubin induced neurotoxicity. The absence of intestinal NF-κB control, known to be regulated by redox changes, has a dramatic impact on UGT1A1 gene expression. Importantly, the direct actions of NF-κB on intestinal UGT1A1 gene expression is independent of TSB levels and the strong antioxidative actions of bilirubin, since deletion of IKKβ in *TgUGT1* mice also leads to developmental reduction in intestinal *UGT1A1* gene expression. Thus, with the intestinal lumen serving as a key reservoir for immediate dietary nutrients through breast feeding, there appears to exist an important balance of oxidative and antioxidative events that impact on regulation of NFκB and *UGT1A1* gene expression. Although it is unclear how intestinal NF-κB control during neonatal development provides downstream signaling events important for regulation of *UGT1A1* gene expression, these findings led us to speculate that more dramatic changes in the redox state of the intestines may influence expression of the *UGT1A1* gene. To consider this possibility, we elected to examine the impact of oral Cd on intestinal *UGT1A1* expression during neonatal development.

We felt that Cd was a good compound to examine its impact on *UGT1A1* gene expression since it does not directly induce oxidative stress, but can disturb the redox state by binding to redox sensitive proteins within the cell such as glutathione [19]. When Cd was given once a day for three days by oral administration starting when the mice were 7 days old, this regiment led to complete reduction in TSB levels in 10-day old *hUGT1/Ikkβ*$^{\Delta IEC}$ and *hUGT1/Ikkβ*$^{F/F}$ mice. Analysis of intestinal and liver *UGT1A1* gene expression demonstrated that Cd induced UGT1A1 only in the small intestines. Interestingly, since the TSB levels were reduced in *hUGT1/Ikkβ*$^{\Delta IEC}$ mice, Cd treatment served to rescue the potential lethality in these mice since they did not develop bilirubin induced neurological toxicity. The ability to reverse the toxicity attributed to the absence of the IKK/NF-κB pathway indicates that NF-κB plays a key role in the endogenous expression pattern of intestinal UGT1A1 but is not crucial when the redox state is dramatically altered as in the case of Cd treatment since induction of UGT1A1 and lowering of TSB levels occurs in both *hUGT1/Ikkβ*$^{\Delta IEC}$ and *hUGT1/Ikkβ*$^{\Delta/F}$ mice. It should also be noted that deletion of IKKβ in mouse embryo fibroblasts [22] and IECs [17] sensitizes these cells to oxidative stress. However, when we examined gene expression patterns linked to either ROS or antioxidant defense mechanism, Cd treatment reduced ROS generated inflammatory markers TNFα and IL-1β, as well as ROS sensitive heme oxygenase-1 (HO-1) expression. The reduction in ROS sensitive genes was paralleled by induction by antioxidant responses as evidenced by induction of *Gsta1* and *Gsta2* gene expression, along with *Cyp2b10*. While *Cyp2b10* can be regulated by the constitutive androstane receptor (CAR), induction of *Cyp2b10* by Cd still occurs in *hUGT1/Car*$^{-/-}$ mice (data not shown), lending support that the potential antioxidant response leading to *Cyp2b10* gene induction by Cd occurs concordantly with that of the *Gsta1, Gsta2* and *UGT1A1* genes.

While Cd produces oxidative stress through indirect processes, As is a direct activator of oxidative stress. When we orally treated *hUGT1/Ikkβ*$^{\Delta IEC}$ and *hUGT1/Ikkβ*$^{F/F}$ mice with As, intestinal *UGT1A1* gene expression was induced followed by a dramatic reduction of TSB. Through examination of transcriptomics by microarray analysis, oxidative responsive sensitive genes such as *Gsta1/Gsta2* are dramatically induced. We also see induction of

Cyp2b10 gene expression, similar to previous experiments following Cd exposure. Gene profiling studies implicate a strong burst in oxidative-reduction mechanisms (Table 1)-confirmed in part by induction of *Cyp* genes-along with induction of gene panels implicating membrane synthesis is being regulated. These findings indicate the insult by As results in the generation of ROS, potentially signaling events to stimulate membrane repair or synthesis. We know from previous findings the *UGT1A1* gene is an Nrf2 target gene induced in response to oxidative stress [32]. The Nrf2/Keap complex is an ROS sensor pathway that when activated leads to induction of genes through ARE responses. Indeed, the *Gst* genes are known targets for Nrf2. However, some of the more dramatically induced genes, such *Cyp4f14, Cyp2b10, Ada*, and *Cox7a* have not been linked to Nrf2 regulation, and the standard target gene for Nrf2 activation, *Nqo1*, is not regulated at all following As treatment. Thus, we cannot dispel the possibility that the impact of ROS is also leading to cell proliferation, which has been confirmed in previous studies [33].

These findings lend support for an important role for NF-κB in control of constitutive expression of the intestinal *UGT1A1* gene during development. During the normal neonatal window there may be an interaction with the components of breast milk and processing of the IKK/NF-κB signaling pathway that is important for constitutive expression of intestinal UGT1A1. The mechanism behind this interaction is unknown. However, in the absence of NF-κB function and a sensitization to oxidative stress [17], mild inflammation in the IECs may be responsible for suppression of intestinal *UGT1A1* gene expression. This inhibition can be overridden by induction of a strong antioxidant response which is generated by Cd or As treatment. How this process leads to induction of intestinal *UGT1A1* gene expression is unknown. It is interesting to note that formula contains a high concentration of unsaturated fatty acids, which may play an important role in modulating the redox state in the intestines following oral feeding. Further studies will be necessary to confirm this response. Thus, the redox-state during development in the intestinal track plays an important role in gene expression, with modulation of the *UGT1A1* gene facilitating the metabolism while controlling levels of TSB during development.

Acknowledgments

This work was supported in part by U.S. Public Health Service Grants ES010337, GM086713, GM100481 (to R.H.T.), R21CA171008 (to S.C.) and R21ES023906 (to M.-F. Yueh). M.L. received a fellowship from the China Scholarship Council which supported in part her research at the UC San Diego.

References

1. Watchko JF. Hyperbilirubinemia and bilirubin toxicity in the late preterm infant. Clin. Perinatol. 2006; 33:839–852. [PubMed: 17148008]
2. Bhutani VK, Maisels MJ, Stark AR, Buonocore G. Management of jaundice and prevention of severe neonatal hyperbilirubinemia in infants ≥35 weeks gestation. Neonatology. 2008; 94:63–67. [PubMed: 18204221]
3. Keren R, Luan X, Friedman S, Saddlemire S, Cnaan A, Bhutani VK. A comparison of alternative risk-assessment strategies for predicting significant neonatal hyperbilirubinemia in term and near-term infants. Pediatrics. 2008; 121:e170–e179. [PubMed: 18166536]
4. Shapiro SM. Chronic bilirubin encephalopathy: diagnosis and outcome. Semin. Fetal Neonatal Med. 2010; 15:157–163. [PubMed: 20116355]

5. Shapiro SM. Bilirubin toxicity in the developing nervous system. Pediatr. Neurol. 2003; 29:410–421. [PubMed: 14684236]
6. Shapiro SM. Definition of the clinical spectrum of kernicterus and bilirubin-induced neurologic dysfunction (BIND). J. Perinatol. 2005; 25(1):54–59. [PubMed: 15578034]
7. Bosma PJ, Seppen J, Goldhoorn B, Bakker C, Oude ER, Chowdhury JR, Chowdhury NR, Jansen PL. Bilirubin UDP-glucuronosyltransferase 1 is the only relevant bilirubin glucuronidating isoform in man. J. Biol. Chem. 1994; 269:17960–17964. [PubMed: 8027054]
8. Fujiwara R, Nguyen N, Chen S, Tukey RH. Developmental hyperbilirubinemia and CNS toxicity in mice humanized with the UDP glucuronosyltransferase 1 (UGT1) locus. Proc. Natl. Acad. Sci. U.S.A. 2010; 107:5024–5029. [PubMed: 20194756]
9. Yueh MF, Chen S, Nguyen N, Tukey RH. Developmental onset of bilirubin-induced neurotoxicity involves Toll-like receptor 2-dependent signaling in humanized UDP-glucuronosyltransferase1 mice. J. Biol. Chem. 2014; 289:4699–4709. [PubMed: 24403077]
10. Chen S, Yueh MF, Evans RM, Tukey RH. The Pregnane-X-receptor controls hepatic glucuronidation during pregnancy and neonatal development in humanized UGT1 mice. Hepatology. 2012; 56:658–667. [PubMed: 22371261]
11. Fujiwara R, Chen S, Karin M, Tukey RH. Reduced expression of UGT1A1 in intestines of humanized UGT1 mice via inactivation of NF-kappa B leads to hyperbilirubinemia. Gastroenterology. 2011; 142:109–118. [PubMed: 21983082]
12. van den Berg R, Haenen GR, van den Berg H, Bast A. Transcription factor NF-kappaB as a potential biomarker for oxidative stress. Br. J. Nutr. 2001; 86(Suppl. 1):S121–S127. [PubMed: 11520430]
13. Chen LW, Egan L, Li ZW, Greten FR, Kagnoff MF, Karin M. The two faces of IKK and NF-kappaB inhibition: prevention of systemic inflammation but increased local injury following intestinal ischemia-reperfusion. Nat. Med. 2003; 9:575–581. [PubMed: 12692538]
14. Fernandes A, Falcao AS, Silva RF, Gordo AC, Gama MJ, Brito MA, Brites D. Inflammatory signalling pathways involved in astroglial activation by unconjugated bilirubin. J. Neurochem. 2006; 96:1667–1679. [PubMed: 16476078]
15. Fernandes A, Silva RF, Falcao AS, Brito MA, Brites D. Cytokinec production glutamate release and cell death in rat cultured astrocytes treated with unconjugated bilirubin and LPS. J. Neuroimmunol. 2004; 153:64–75. [PubMed: 15265664]
16. Janssen-Heininger YM, Poynter ME, Baeuerle PA. Recent advances towards understanding redox mechanisms in the activation of nuclear factor kappaB. Free Radic. Biol. Med. 2000; 28:1317–1327. [PubMed: 10924851]
17. Eckmann L, Nebelsiek T, Fingerle AA, Dann SM, Mages J, Lang R, Robine S, Kagnoff MF, Schmid RM, Karin M, Arkan MC, Greten FR. Opposing functions of IKKbeta during acute and chronic intestinal inflammation. Proc. Natl. Acad. Sci. U.S.A. 2008; 105:15058–15063. [PubMed: 18815378]
18. Shibata W, Takaishi S, Muthupalani S, Pritchard DM, Whary MT, Rogers AB, Fox JG, Betz KS, Kaestner KH, Karin M, Wang TC. Conditional deletion of IkappaB-kinase-beta accelerates helicobacter-dependent gastric apoptosis proliferation and preneoplasia. Gastroenterology. 2010; 138:1022–1034. [PubMed: 19962981]
19. Cuypers A, Plusquin M, Remans T, Jozefczak M, Keunen E, Gielen H, Opdenakker K, Nair AR, Munters E, Artois TJ, Nawrot T, Vangronsveld J, Smeets K. Cadmium stress: an oxidative challenge. Biometals. 2010; 23:927–940. [PubMed: 20361350]
20. Lopez E, Arce C, Oset-Gasque MJ, Canadas S, Gonzalez MP. Cadmium induces reactive oxygen species generation and lipid peroxidation in cortical neurons in culture. Free Radic. Biol. Med. 2006; 40:940–951. [PubMed: 16540389]
21. Peng Z, Geh E, Chen L, Meng Q, Fan Y, Sartor M, Shertzer HG, Liu ZG, Puga A, Xia Y. Inhibitor of kappaB kinase beta regulates redox homeostasis by controlling the constitutive levels of glutathione. Mol. Pharmacol. 2010; 77:784–792. [PubMed: 20159942]
22. Chen F, Castranova V, Li Z, Karin M, Shi X. Inhibitor of nuclear factor kappaB kinase deficiency enhances oxidative stress and prolongs c-Jun NH_2-terminal kinase activation induced by arsenic. Cancer Res. 2003; 63:7689–7693. [PubMed: 14633691]

23. Santra A, Maiti A, Chowdhury A, Mazumder DN. Oxidative stress in liver of mice exposed to arsenic-contaminated water. Indian J. Gastroenterol. 2000; 19:112–115. [PubMed: 10918716]
24. Ercal N, Gurer-Orhan H, Aykin-Burns N. Toxic metals and oxidative stress part I: mechanisms involved in metal-induced oxidative damage. Curr. Top. Med. Chem. 2001; 1:529–539. [PubMed: 11895129]
25. Li M, Cai JF, Chiu JF. Arsenic induces oxidative stress and activates stress gene expressions in cultured lung epithelial cells. J. Cell. Biochem. 2002; 87:29–38. [PubMed: 12210719]
26. Liu L, Trimarchi JR, Navarro P, Blasco MA, Keefe DL. Oxidative stress contributes to arsenic-induced telomere attrition chromosome instability and apoptosis. J. Biol. Chem. 2003; 278:31998–32004. [PubMed: 12767976]
27. Nguyen N, Bonzo JA, Chen S, Chouinard S, Kelner M, Hardiman G, Belanger A, Tukey RH. Disruption of the *Ugt1* locus in mice resembles human Crigler-Najjar type I disease. J. Biol. Chem. 2008; 283:7901–7911. [PubMed: 18180294]
28. Barateiro A, Chen SJ, Yueh MF, Fernandes A, Domingues HS, Relvas J, Barbier O, Nguyen N, Tukey RH, Brites D. Reduced myelination and increased glia reactivity resulting from severe neonatal hyperbilirubinemia. Mol. Pharmacol. 2015
29. Cai H, Nguyen N, Peterkin V, Yang YS, Hotz K, Beaton La PD, Chen S, Tukey RH, Stevens JC. A humanized *UGT1* mouse model expressing the *UGT1A1*28* allele for assessing drug clearance by UGT1A1 dependent glucuronidation. Drug Metab. Dispos. 2010; 38:879–886. [PubMed: 20124398]
30. Chen S, Yueh MF, Bigo C, Barbier O, Wang K, Karin M, Nguyen N, Tukey RH. Intestinal glucuronidation protects against chemotherapy-induced toxicity by irinotecan (CPT-11). Proc. Natl. Acad. Sci. U.S.A. 2013; 110:19143–19148. [PubMed: 24191041]
31. Spehlmann ME, Eckmann L. Nuclear factor-kappa B in intestinal protection and destruction. Curr. Opin. Gastroenterol. 2009; 25:92–99. [PubMed: 19528876]
32. Yueh MF, Tukey RH. Nrf2-Keap1 signaling pathway regulates human *UGT1A1* expression in vitro and in transgenic UGT1 mice. J. Biol. Chem. 2007; 282:8749–8758. [PubMed: 17259171]
33. Qian Y, Castranova V, Shi X. New perspectives in arsenic-induced cell signal transduction. J. Inorg. Biochem. 2003; 96:271–278. [PubMed: 12888263]
34. Cole SW, Galic Z, Zack JA. Controlling false-negative errors in microarray differential expression analysis: a PRIM approach. Bioinformatics. 2003; 19:1808–1816. [PubMed: 14512352]

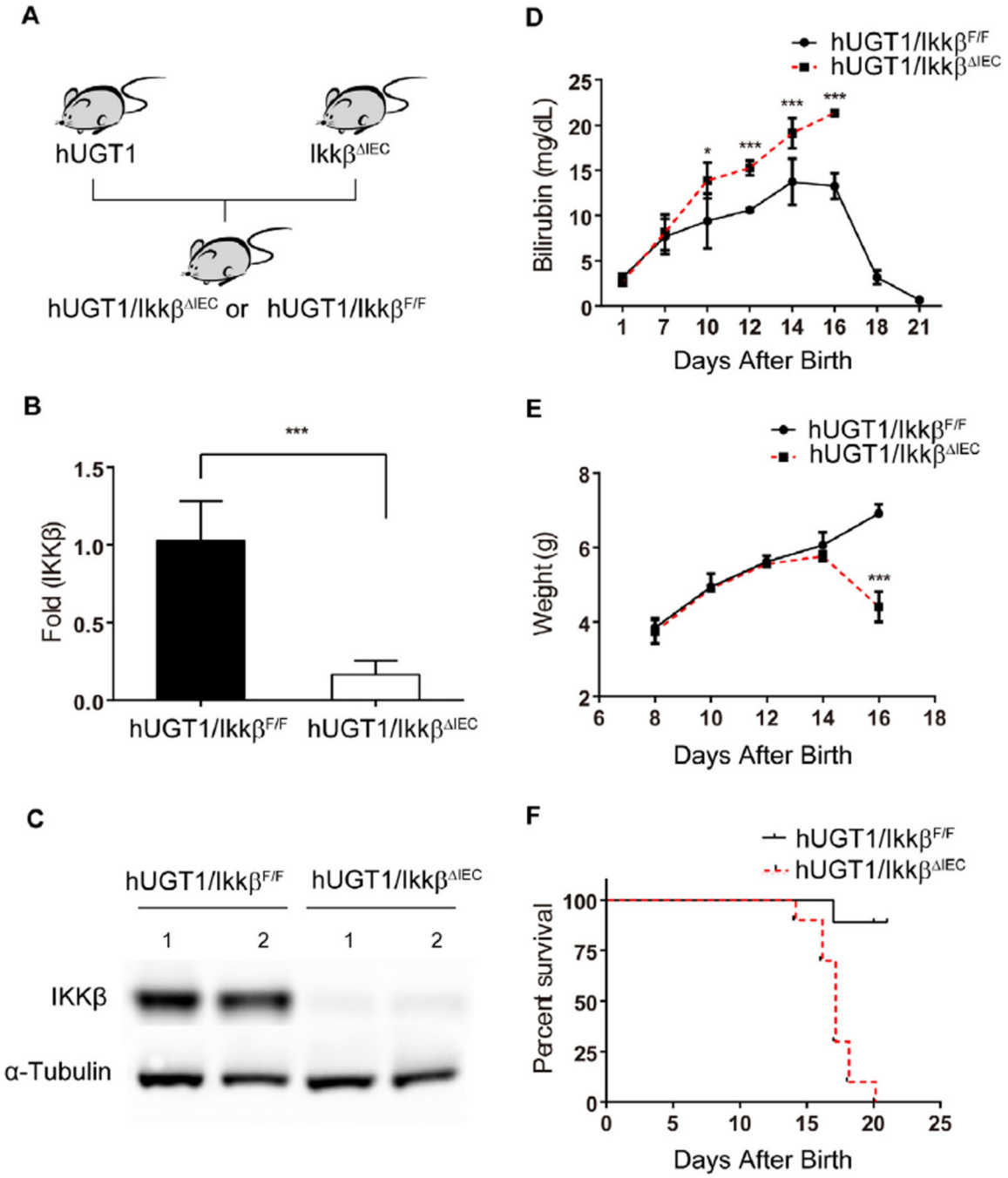

Fig. 1.

Neonatal *hUGT1/Ikkβ$^{\Delta IEC}$* mice develops lethal hyperbilirubinemia. (A) The generation of humanized *UGT1/Ikkβ$^{F/F}$/villin-Cre* mice (*hUGT1/Ikkβ$^{\Delta IEC}$* mice) and their littermate control *hUGT1/Ikkiβ$^{F/F}$* mice. (B) Intact IKKβ mRNA and (C) protein levels in the small intestine of *hUGT1/Ikkβ$^{\Delta IEC}$* and *hUGT1/Ikkβ$^{F/F}$* mice. (D) Serum bilirubin levels of *hUGT1/Ikkβ$^{\Delta IEC}$* and *hUGT1/Ikkβ$^{F/F}$* mice during their infantile stage. (E) Weight development of *hUGT1/Ikkβ$^{\Delta IEC}$* and *hUGT1/Ikkβ$^{F/F}$* mice from day 8 to day 16. At least four mice were analyzed in each group or time point. (F) Survival rate of *hUGT1/Ikkβ$^{\Delta IEC}$*

and *hUGT1/Ikkβ*$^{F/F}$ mice during their infantile stage. The Kaplan–Meier estimator used to predict survival estimates consisted of over 50 mice from multiple litters per strain. The results are presented as mean ± SD ($^{*}P < 0.05$, $^{***}P < 0.005$).

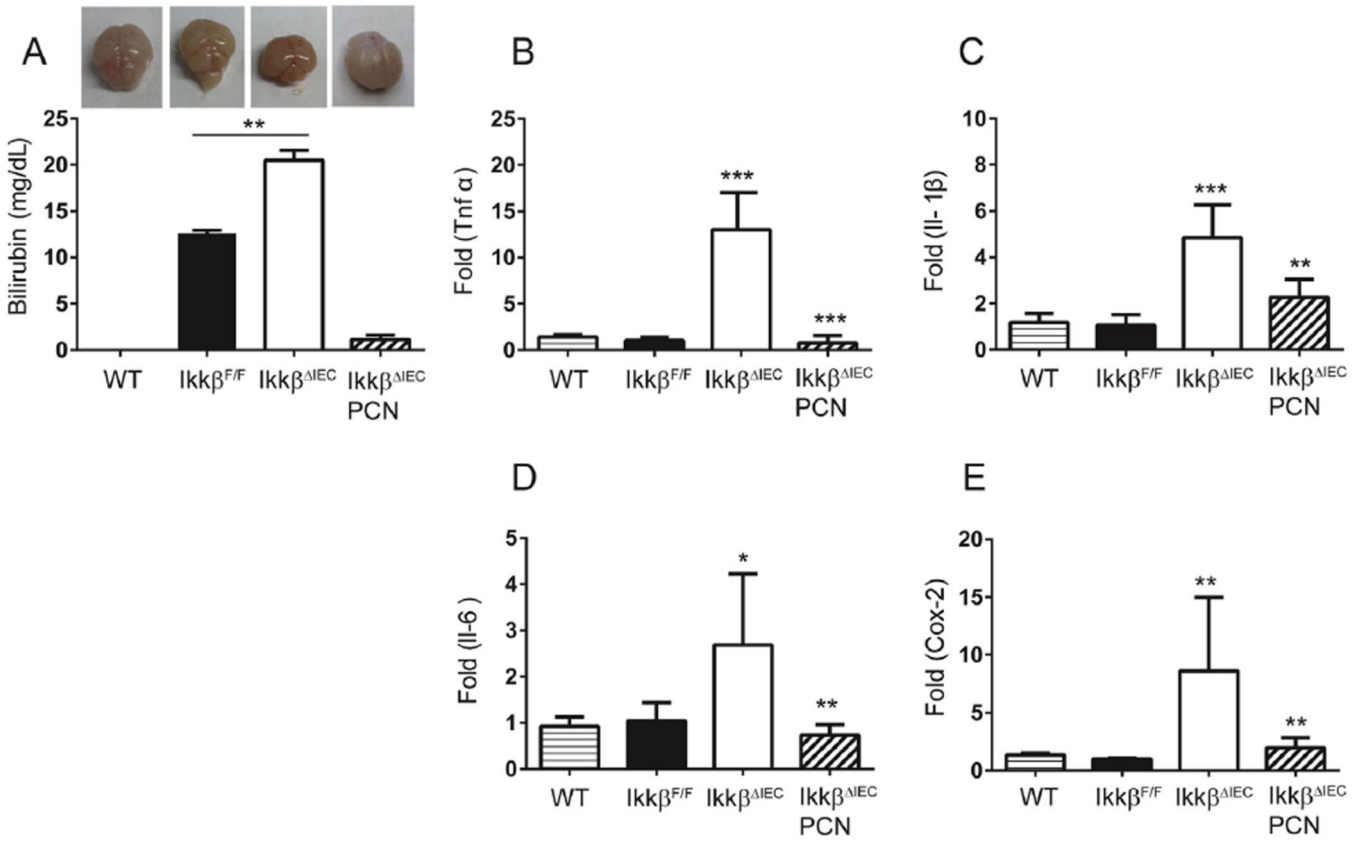

Fig. 2.

Severe hyperbilirubinemia causes UCB accumulation and dramatic inflammatory response in the brain of *hUGT1/Ikkβ*$^{\Delta IEC}$ mice. Mouse blood and brains were collected from 15-day old wild type (WT), *hUGT1/Ikkβ*$^{F/F}$ (Ikkβ$^{F/F}$), *hUGT1/Ikkβ*$^{\Delta IEC}$ (Ikkβ$^{\Delta IEC}$) and PCN treated *hUGT1/Ikkβ*$^{\Delta IEC}$ (Ikkβ$^{\Delta IEC}$) mice. (A) Mouse total serum bilirubin levels. Shown above each bar graph is a representation of mouse brain from wild type, mild jaundiced *hUGT1/Ikkβ*$^{F/F}$, severe jaundiced *hUGT1/Ikkβ*$^{\Delta IEC}$, and PCN treated *hUGT1/Ikkβ*$^{\Delta IEC}$ mice. (B–E) Expression of pro-inflammatory markers in mouse brain. At least four mice were analyzed in each group and results are presented as mean ± SD ($^{*}P < 0.05$, $^{**}P < 0.01$, $^{***}P < 0.005$).

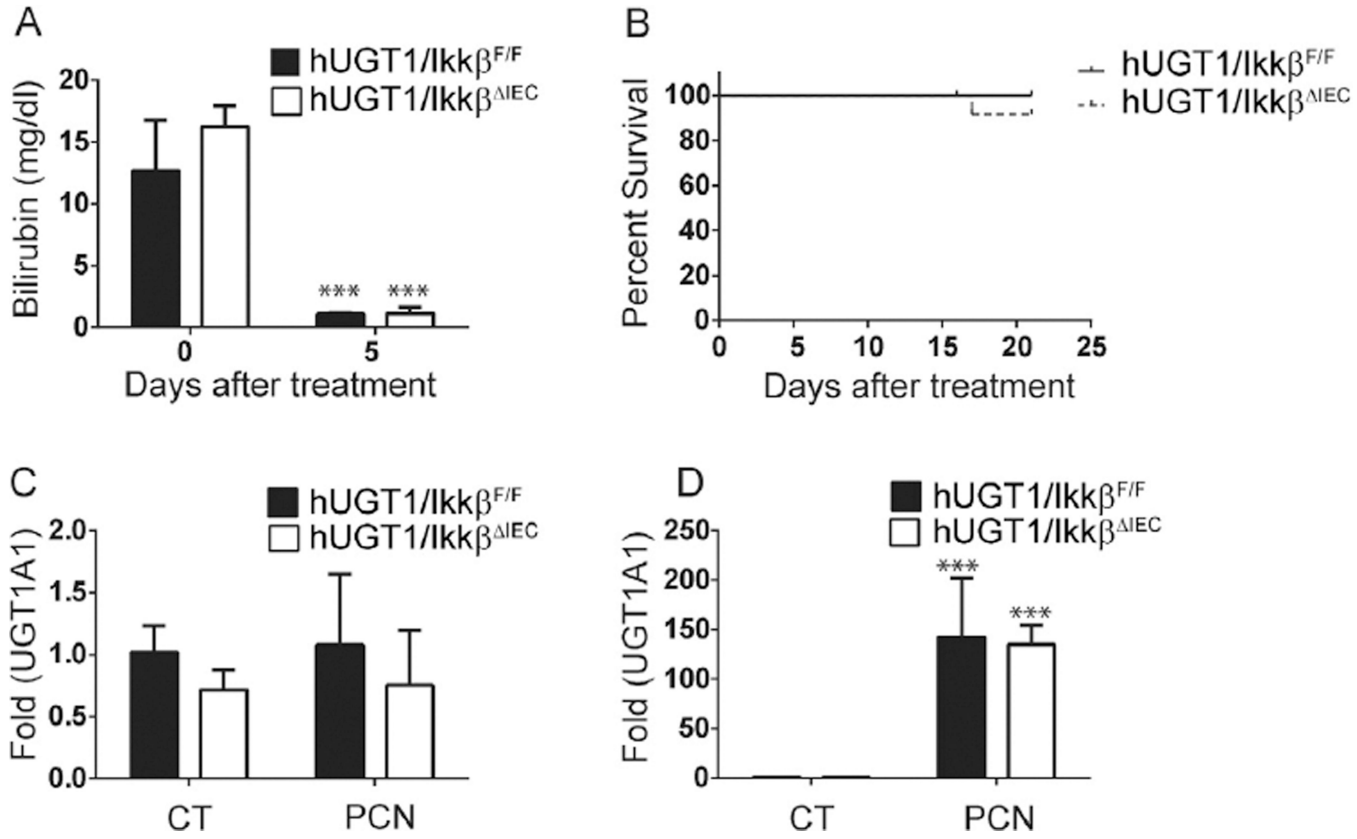

Fig. 3.

hUGT1/Ikkβ$^{\Delta IEC}$ mice can be rescued by PCN induced liver UGT1A1 expression. 11-day old *hUGT1/Ikkβ*$^{\Delta IEC}$ and *hUGT1/Ikkβ*$^{F/F}$ mice were orally treated with vehicle control (CT) or PCN (10 mg/kg) every 24 h over a 3-day period. 2 days after the last treatment, samples were collected and analyzed. (A) Serum total bilirubin levels of *hUGT1/Ikkβ*$^{\Delta IEC}$ and *hUGT1/Ikkβ*$^{F/F}$ mice before and after PCN treatment. (B) Kaplan–Meier survival rate of *hUGT1/Ikkβ*$^{\Delta IEC}$ and *hUGT1/Ikkβ*$^{F/F}$ mice treated with PCN (10 mg/kg) at 8–10 days of age. Over 20 mice from each strain were treated with PCN. (C) Small intestinal and (D) hepatic UGT1A1 mRNA levels of *hUGT1/Ikkβ*$^{\Delta IEC}$ and *hUGT1/Ikkβ*$^{F/F}$ mice with or without PCN treatment. In A, C and D at least four mice were analyzed in each group and results presented as mean ± SD ($^{***}P < 0.005$).

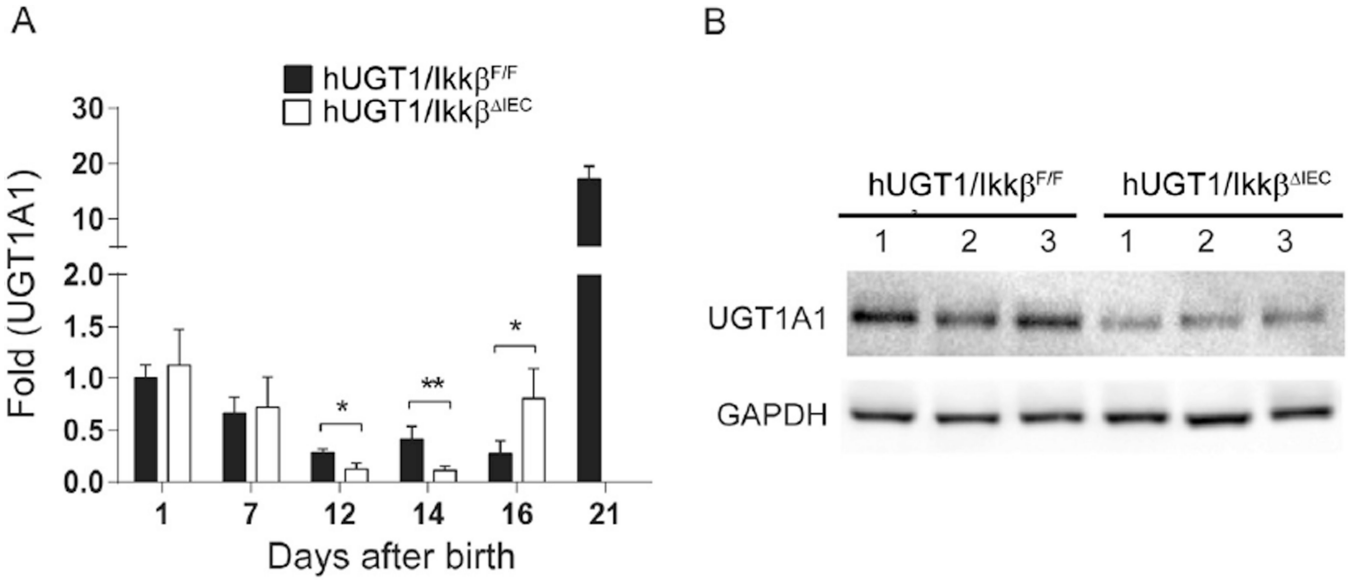

Fig. 4.

IKKβ knock-out in the IECs inhibits intestinal human UGT1A1 expression in neonatal *hUGT1/Ikkβ*$^{\Delta IEC}$ mice. (A) Small intestinal UGT1A1 mRNA levels of neonatal *hUGT1/Ikkβ*$^{\Delta IEC}$ and *hUGT1/Ikkβ*$^{F/F}$ mice. (B) Small intestinal UGT1A1 protein levels of 14-day old *hUGT1/Ikkβ*$^{\Delta IEC}$ and *hUGT1/Ikkβ*$^{F/F}$ mice. Three to five mice were analyzed in each group and results are presented as mean ± SD ($^{*}P < 0.05$, $^{**}P < 0.01$).

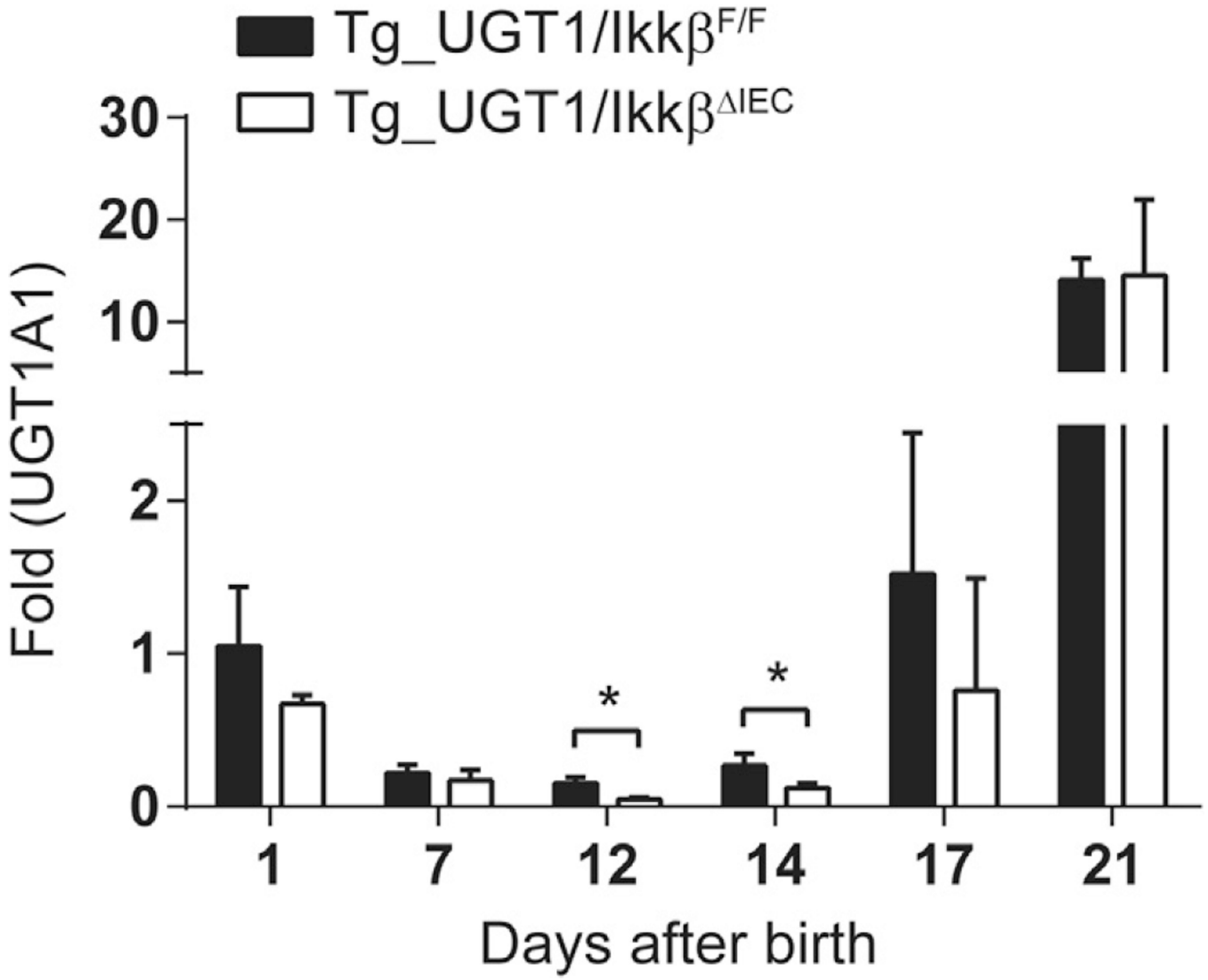

Fig. 5.

IKKβ knock-out in the IECs inhibits intestinal human UGT1A1 expression in neonatal *Tg_UGT1/Ikkβ*$^{\Delta IEC}$ mice. Small intestinal UGT1A1 mRNA levels of neonatal *TgUGT1/Ikkβ*$^{\Delta IEC}$ and *Tg_UGT1/Ikkβ*$^{F/F}$ mice were detected by real time PCR. At least three mice were analyzed in each group and results are presented as mean ± SD (*$P < 0.05$).

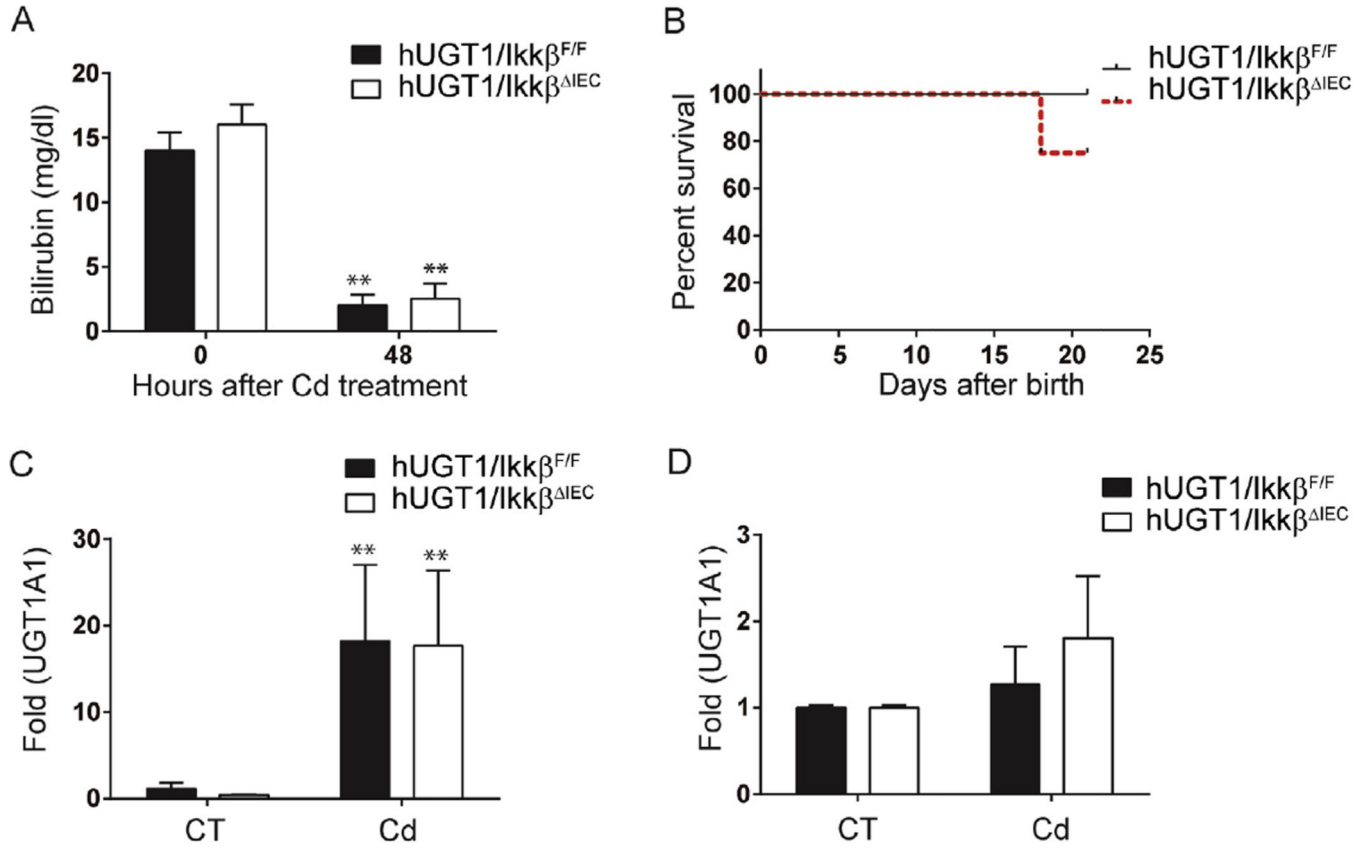

Fig. 6.

Cadmium can equally induce small intestinal UGT1A1 expression in *hUGT1/Ikkβ*$^{\Delta IEC}$ and *hUGT1/Ikkβ*$^{F/F}$ mice. 10-day old *hUGT1/Ikkβ*$^{\Delta IEC}$ and *hUGT1/Ikkβ*$^{F/F}$ mice were treated with vehicle control (CT) or cadmium chloride hemipentahydrate (Cd, 10 mg/kg) orally. 48 h after the treatment, samples were collected and analyzed. (A) Total serum bilirubin levels of *hUGT1/Ikkβ*$^{\Delta IEC}$ and *hUGT1/Ikkβ*$^{F/F}$ mice before and after Cd treatment. (B) Survival rate of *hUGT1/Ikkβ*$^{\Delta IEC}$ and *hUGT1/Ikkβ*$^{F/F}$ mice treated with Cd. Approximately 40 mice of each strain were treated with Cd. (C) Small intestinal and (D) hepatic UGT1A1 mRNA levels of *hUGT1/Ikkβ*$^{\Delta IEC}$ and *hUGT1/Ikkβ*$^{F/F}$ mice with or without Cd treatment. At least four mice were analyzed in each group and results are presented as mean ± SD ($^{**}P < 0.01$).

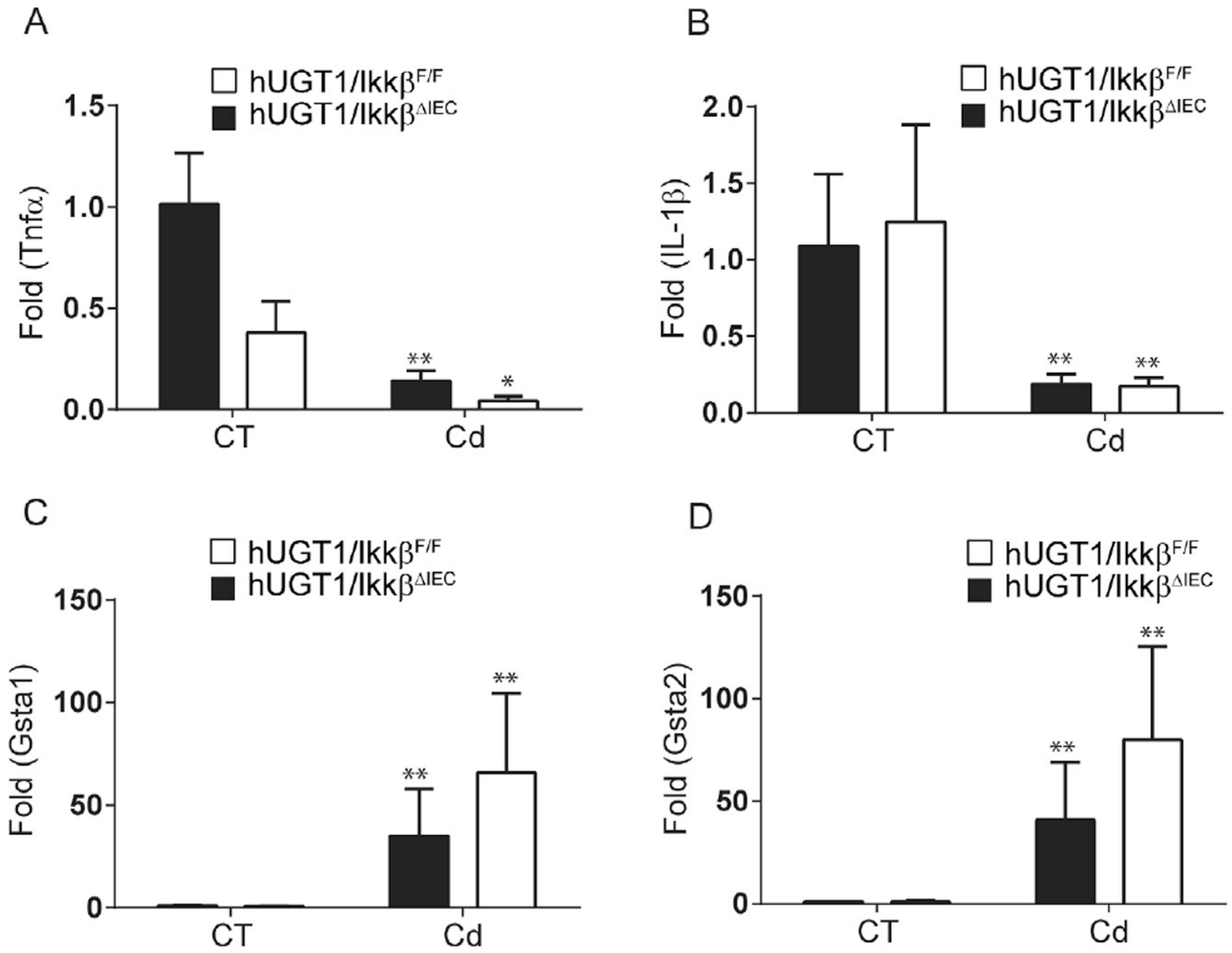

Fig. 7.

Cadmium exposure can lead to the activation of antioxidative mechanisms in *hUGT1/Ikkβ$^{\Delta IEC}$* and *hUGT1/Ikkβ$^{F/F}$* mice. 10-day old *hUGT1/Ikkβ$^{\Delta IEC}$* and *hUGT1/Ikkβ$^{F/F}$* mice were treated with vehicle control (CT) or cadmium chloride hemipentahydrate (Cd, 10 mg/kg) orally. 48 h after the treatment, samples were collected. Small intestinal (A) TNFα, (B) IL-1β, (C) GSTA1 and (D) GSTA2 mRNA levels were analyzed by real time PCR. At least three mice were analyzed in each group and results are presented as mean ± SD ($^{*}P < 0.05$, $^{**}P < 0.01$, $^{***}P < 0.005$).

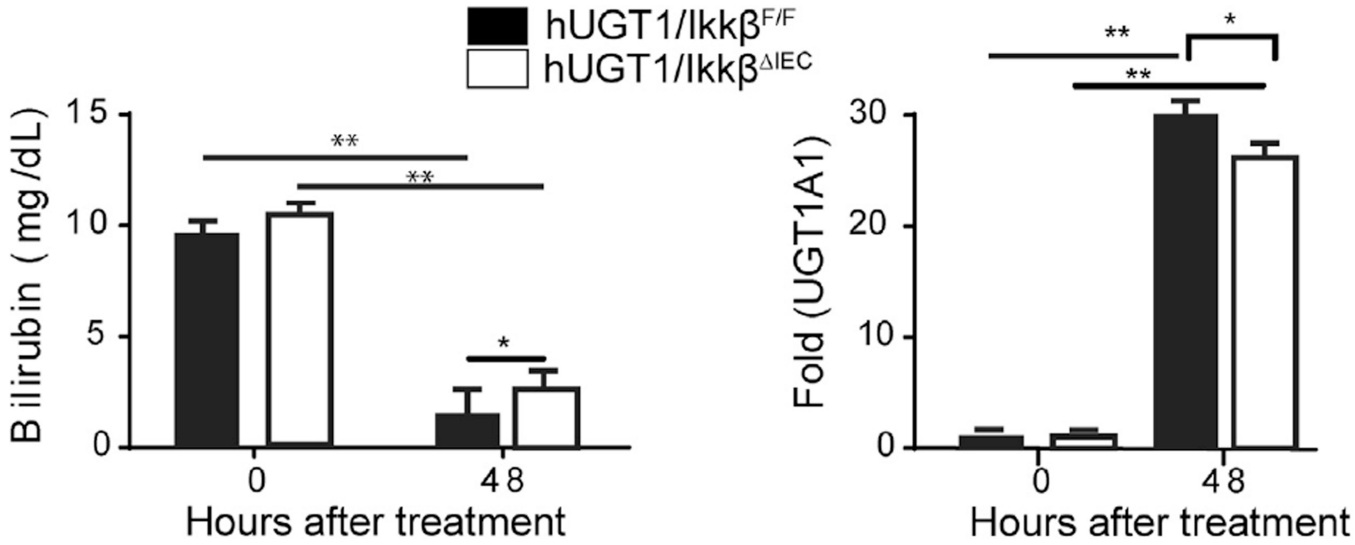

Fig. 8.

Oral arsenic (As) induces intestinal UGT1A1. 10-day old *hUGT1/Ikkβ*$^{\Delta IEC}$ and *hUGT1/Ikkβ*$^{F/F}$ mice were treated with vehicle control (CT) or arsenic (As-1 mg/kg) orally. 48 h after the treatment, serum bilirubin levels were measured along with *UGT1A1* gene expression from small intestinal tissue. Five to 8 mice were analyzed in each treatment group and the results presented as mean ± SD ($^{*}P < 0.05$, $^{**}P < 0.01$).

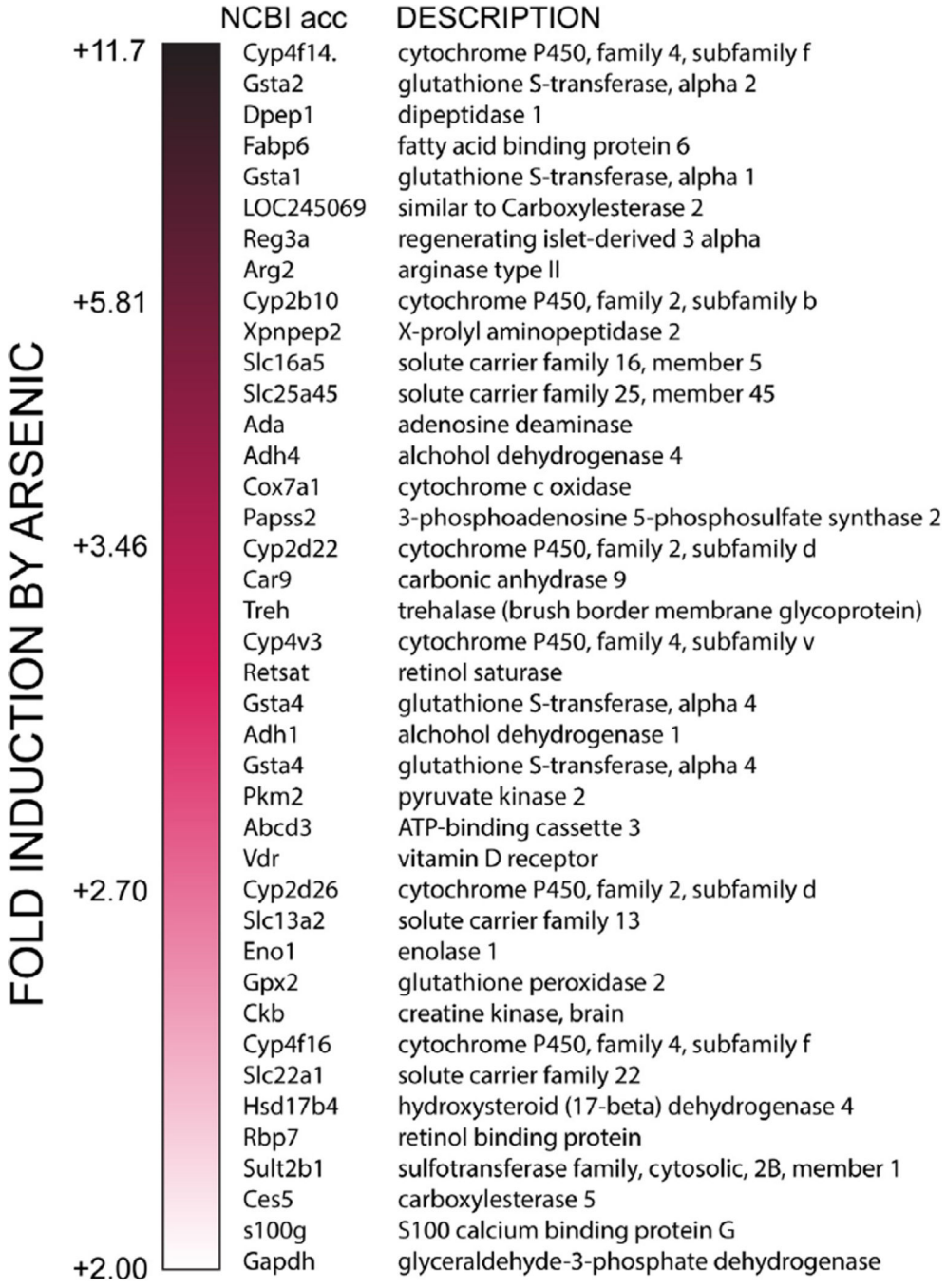

Fig. 9.

Microarray analysis. Total RNA from 12-day old *hUGT1* mice treated orally with 1 mg/kg As for 48 h was isolated along with vehicle treated *hUGT1* mice and used in microarray studies. Using the Illumina Mouse Sentrix Expression BeadChip, the expression of each gene in either vehicle or arsenic treated mice was analyzed by averaging 5 independent RNA samples from each group. Shown is a heat map of some of the genes that are upregulated at >2 fold.

Table 1

List of functional pathways that are altered significantly in arsenic treated *hUGT1* neonatal small intestine compared to untreated *hUGT1* mice.

Pathway description	*P* value
Oxidation-reduction process	5.62E-23
Carboxylic acid metabolic process	3.95E-20
Lipid metabolic process	9.45E-20
Oxoacid metabolic process	4.15E-19
Organic acid metabolic process	9.12E-19
Cellular lipoid metabolic process	2.17E-17
Monocarboxylic acid metabolic process	5.46E-16
Fatty acid metabolic process	9.51E-13
Cofactor metabolic process	7.72E-12
Lipid catabolic process	2.22E-10

In ranking genes we utilized the method described by Cole et al. [34]. The pathways included are all those listed in the *Kyoto Encyclopedia of Genes and Genomes*. As the P values increase, the pathways become less and less significant. Shown are some of the pathways with a *P* value $<10^{-9}$.